MAUSAM, **63**, 1 (January 2012), 77-88

551. 501.86

IPWV estimation and data quality analysis from different GNSS antenna

J. K. S. YADAV, R. K. GIRI and L. R. MEENA

India Meteorological Department, New Delhi, India

(*Received 15 April 2010, Modified 10 January 2011*)

e mail : jksmet@gmail.com

सार – वैश्विक संचालन उपग्रह तंत्र (जी. एन. एस. एस.) का आजकल अनेक अनुप्रयोगों में काफी उपयोग हो रहा है। धरातल आधारित अभिग्राही में प्राप्त समाकलित वर्षणीय जल वाष्प (आई. पी. डब्ल्यू. वी.) के लगभग वास्तविक समय आकलन के लिए प्रेक्षण फाइल में अस्पष्टता रहती है। बहु–पथ प्रभाव तंत्र, सिस्टम के ध्रातल पर लगे अभिग्राही से उपग्रह तक स्थैतिक सटीकता और अवधि को प्रभावित करता है। एंटीना का डिजाइन बहु–पथ, साइकल स्लिप्स, प्रेक्षणों की संख्या, सिग्लन की तीव्रता और डाटा स्ट्रीम्स में निहित डाटा गैप्स के प्रभाव को कम करता है। इस शोध पत्र में पैच एंटीना (लेका X1202) 3 डी. चोक रिंग एंटीना (लेका ए. आर. 25 जी. एन. एस. एस.) और ट्रिम्बल जैफिर एंटीना (टी. आर. एम. 39105.00) के आरंभिक आँकड़ा गुणवत्ता नियंत्रण के निष्कर्षों को प्रस्तुत किया गया है। इन निष्कर्षों से प्राप्त हुए परिणामों से पता चलता है कि आई. पी. डब्ल्यू. वी. में सुधार के साथ–साथ चोक रिंग एंटीना में आँकड़ों, साइकल स्लिप्स और बहु–पथ प्रभावों में बहुत कम गैप्स रहे। 3 डी. चोक रिंग एंटीना के मामले में सिग्लन तीव्रता और प्रेक्षणों की संख्या अधिक रही।

ABSTRACT. Global Navigation Satellite System (GNSS) is widely used now days in variety of applications. The observation file for the near realtime estimation of Integrated Precipitable Water Vapour (IPWV) received at the ground-based receiver is mixed with ambiguities. Multi-path effects affect the positional accuracy as well as range from satellite to ground based receiver of the system. The designing of the antenna suppress the effect of multi-path, cycle slips, number of observations, and signal strength and data gaps within the data streams. This paper presents the preliminary data quality control findings of the Patch antenna (LeicaX1202), 3D Choke ring antenna (LeicaAR25 GNSS) and Trimble Zephyr antenna (TRM 39105.00). The results shows that choke ring antenna have least gaps in the data, cycle slips and multi-path effects along with improvement in IPWV. The signal strength and the number of observations are more in case of 3D choke ring antenna.

Key words – GNSS, Cycle slip, Signal to noise ratio (SNR), Choke ring antenna and Multi-path.

1. Introduction

An antenna's job is to capture some of the power in the electromagnetic waves it receives and to convert it into an electrical current that can be processed by the receiver. With very strong signals at lower frequencies, almost any kind of antenna will serve the purpose. In general, an antenna must be designed for the particular signals to be intercepted, with the center frequency, bandwidth, and polarization of the signals being important parameters in the design. As the required receiver position fixes accuracy approaches centimeter and even sub-centimeter levels, the demands on the antenna increase, with multi-path suppression and phase-center stability becoming important characteristics. Various properties and trade-offs that affect functionality and performance of the antenna are different for different antennas. For the precise estimation of Integrated Precipitable Water Vapour (IPWV) both the Global Navigation Satellite System (GNSS) receiver and antenna are equally important. The coverage of the frequencies used by these systems are unique, such as Galileo's E6 band and the GLONASS L1 band, and may not be covered by all antennas. GPS satellites transmit the radio signal, which travels through different layers of the atmosphere. The troposphere part is mainly responsible for weather, and satellite signals pass in layers of varying refractive indices, the refractivity profile can be transformed to profiles of tropospheric humidity by using the thermodynamical relationships.

In the existing operationally running system signal emanating from the GPS satellites is captured by Leica X1202 (Patch antenna) and received in Leica GRX 1200 receiver. The RINEX hourly data from five GPS stations (Delhi, Mumbai, Kolkata, Chennai and Guwahati) are being processed near real time basis centrally at Delhi. Daily at each site Leica binary observation file are stored both on the receiver-internal Compact flash card (in ring buffer mode) and externally on the data logging PC. The Leica binary observation files of the logging PC are automatically converted into RINEX format through spider software. The RINEX zip file contains three files namely; observation, navigation (broadcast ephemeris) and meteorological data, archived and final product Integrated Precipitable Water Vapour (IPWV) is uploaded to India Meteorological Department (IMD) web site and made available to the end users. The near real time and post processing of the observational data is also done by the GAMIT 10.3.2.1 processing software. Leica GRX 1200 is a dual frequency (with fully independent L1 and L2 tracking loops) receiver. Similar, structure of data was made available with Trimble Zephr (TRM39105.00) and Leica 3D chokering (Leica AR25GNSS) antenna system and processed with GAMIT 10.3.2.1 software. The final IPWV estimation could not be done with Trimble Zephr antenna due to incompatibility of various modules in GAMIT processing. Although the data quality of Trimble Zephr antenna is checked by TEQC utility. In General, the functionality and performance of the GNSS antenna depends mainly on the following properties:

- Frequency coverage
- Gain pattern
- Circular polarization
- Multipath suppression
- Phase center
- Impact on receiver sensitivity
- Interference handling

Multi-constellation bands compatibility of the GNSS receivers makes the antenna design harder and developing an antenna that covers all of these bands and match with all of the other requirements is a challenge.

2. Data and Methodology

For the present study the Receiver Independent Exchange (RINEX) Format data for the three type of antenna has been obtained from India Meteorological Department Lodi Road New Delhi. They are Patch antenna (LeicaX1202), 3 D Choke ring antenna (LeicaAR25 GNSS) and Trimble Zephyr antenna, (TRM 39105.00). The existing five GPS systems are working with Patch antenna LeicaX1202 receiver. Other two antennas have been installed at Mausam Bhawan, Lodi Road, New Delhi for almost 20 days (07 July 2009 to 25 July 2009). The RINEX data is collected for all the three systems and finally processed by two systems LeicaX1202 and LeicaAR25 GNSS receivers. For quality control analysis of Trimble Zephyr and LeicaAR25 antennas observations files the Leica GNSS QC V 2.1.2 software (Estey and Meertens, 1999) has been used. The observation data received from patch and choke ring antenna is processed independently through GAMIT 10.3.2 software for IPWV estimation. For the existing old LeicaAX1202, TEQC tool kit software developed by University NAVSTAR Consortium (UNAVCO) Boulder, USA has been used. For comparison of data quality we have taken the data of 29 July 2009 (0530 UTC to 0620 UTC) for all the three systems.

2.1. *Retrieval procedure for IPWV estimation*

Ground based GPS systems are used for the estimation of Integrated Precipitable water vapour (IPWV). It is measured by computing the delay in GPS signals due to the moisture present in the atmosphere. The main sources of delay in GPS dual frequency radio signals (L1=1575 Mhz, L2 = 1225 Mhz) are Ionosphere and Troposphere. The Ionosphere delay or error is removed by the linear combination of L1 and L2 frequencies. But Troposphere delay cannot be removed easily. The total delay in the Zenith direction is estimated with the help of GPS observational data. The total delay in zenith direction (ZTD) is the sum of two parts; dry delay in zenith direction called zenith hydrostatic delay (ZHD) and wet delay, which is known as zenith wet delay (ZWD). ZTD values are estimated from the observation file getting from the GPS receiver of each site by measuring the pseudo range or phase delay methods .The brief computation procedure of estimation of Integrated Precipitable Water Vapour (IPWV) is given below:

$$ZTD = ZHD + ZWD$$

ZHD values are more sensitive to station level pressure and temperature and calculated by the following formula:

$$ZHD = 0.00278 * P_s * [1 + 0.0026 * \cos(2\phi) + 0.00000028 * H_s]$$

Where,

Ps = Station level pressure in milibar

TABLE 1

Code Multi-path RMS by satellite (+) & Average Signal Strength by PRN (*) for Leica Choke ring (LeicaAR25 GNSS) Antenna

Satellite vehicle (SV)	Av Elev (degree)	MP1 (mm)	MP2 (mm)	Average Signal Strength (SNR)** L1	Average Signal Strength (SNR)** L2
G3	11.7	0.14	0.25	4.2	7.9
G6	14.1	0.18	0.17	4.5	6.8
G9	09.4	0.24	0.30	6.7	6.8
G14	63.1	0.13	0.08	9.0	8.5
G18	33.0	0.22	0.23	8.6	1.5
G19	17.7	0.22	0.20	5.7	2.3
G21	12.3	0.25	0.27	4.7	5.8
G22	56.9	0.11	0.08	1.3	8.9
G26	28.4	0.14	0.13	8.0	2.7
G31	36.6	0.20	0.14	8.4	5.1

** Signal strength is mapped between 1 (worst) and 9 (best), 5 is the threshold for good SNR, 0 indicates value is unknown

TABLE 2

Code Multi-path RMS by satellite (+) & Average Signal Strength by PRN (*) for Trimble Zephyr antenna (TRM 39105.00)

Satellite vehicle (SV)	Av Elev	MP1 (mm)	MP2 (mm)	Average Signal Strength (SNR) L1	Average Signal Strength (SNR) L2
G3	11.7	0.00	0.56	40.2	22.0
G6	14.1	0.52	0.45	40.1	22.6
G9	09.4	0.35	0.00	41.2	23.8
G14	63.1	0.20	0.12	35.1	17.4
G18	33.0	0.20	0.47	40.2	23.1
G19	17.7	0.21	0.34	49.6	39.1
G21	15.3	0.38	0.00	42.5	23.6
G22	56.9	0.20	0.14	51.6	40.7
G26	28.4	0.35	0.35	45.1	31.5
G31	36.6	0.48	0.21	47.3	34.2

Hs = Surface height above geoid in km

ϕ = Latitude of the station

PWV = K* ZWD

Where,

$$K = \left\{ 10^{-6} \left(\frac{k_3}{T_m} + k_2 \right) R_v \rho \right\}^{-1}$$

ρ = Density of water in Kg/m^3

Where,

k_2 = (17 ± 10) Kmb^{-1},

k_3 = (3.776 ± 0.004) 10^5 K^2 mb^{-1}

Rv = water vapour gas constant

*T*m = weighed mean temperature of the atmosphere is given by

TABLE 3

Code Multi-path RMS by satellite (+) & Average Signal Strength by PRN (*) for Patch antenna (LeicaX1202)

Satellite vehicle (SV)	Av Elev	MP1 (mm)	MP2 (mm)	Average Signal Strength (SNR) L1	Average Signal Strength (SNR) L2
G3	11.7	0.00	0.56	49.33	43.32
G6	14.1	0.52	0.45	49.63	42.80
G9	09.4	0.35	0.00	49.16	42.02
G14	63.1	0.20	0.12	48.83	39.89
G18	33.0	0.20	0.47	47.89	38.22
G19	17.7	0.21	0.34	40.30	36.26
G21	15.3	0.38	0.00	35.72	32.58
G22	56.9	0.20	0.14	44.26	30.59
G26	28.4	0.35	0.35	46.29	33.21
G31	36.6	0.48	0.21	37.43	41.27

Note : Abbreviations: Av = Average, IOD = Ionospheric delay, Num = Number, Obs = Observations, MP = Multipath, SV = Satellite vehicle, Slips = Cycle slips

TABLE 4

Comparison of different parameters of antennas

Name of the Antenna → / Parameters ↓	3D- Choke ring antenna (LeicaAR25 GNSS)	Trimble Zephyr antenna (TRM 39105.00)	Patch antenna (LeicaX1202)
Data gaps (time)	0.0 (5 second)*	3.0 minute (5 second)*	4.0 minute (5 second)*
Average of PDOP	4.8	4.8	5.8
Average of GDOP	5.7	5.7	6.2
SV (average number)	7.2	7.2	5.4
MP1 RMS (m)	0.16 (0.5)*	0.26	0.26
MP2 RMS (m)	0.17 (0.5)*	0.24	0.38
Total cycle Slips (number)	0 (2)*	11 (2)*	12
Clock offsets (millisecond)	0.00025	0.00019	0.00012
L1 (SNR) (average)	7.0	44.9	47.7
L2 (SNR) (average)	5.4	29.7	39.5
EPOCH	100% (99)*	95.8% (99)*	95.2% (99)*

* Values in the above table are threshold values to pass the quality test.

$T_m = 55.8\ (°K) + 0.77 * T_s\ (°K)$

T_s = Surface temperature

ZHD values can be modeled properly and ZWD values cannot be modeled properly due to its in homogeneity in space and time. The final output product of precipitable water will be in mm. Its estimation from GPS is more precise and timely which is very useful in assimilating it into numerical models to modify the moisture fields.

3. Discussion

The preliminary results obtained by using the above said software for Patch antenna (LeicaX1202), Choke ring

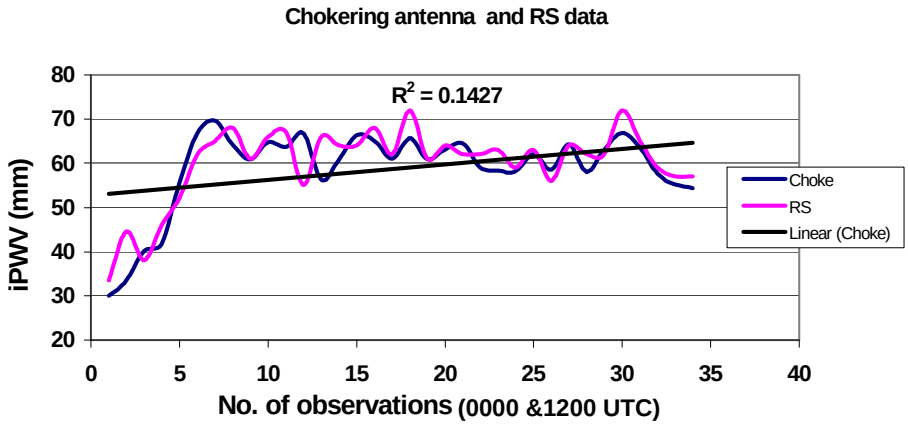

Fig. 1. IPWV (mm) processing results by Choke-ring antenna with RS data

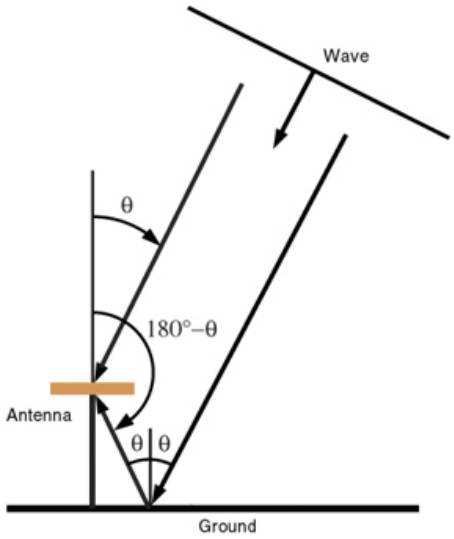

Fig. A. Reflections from ground

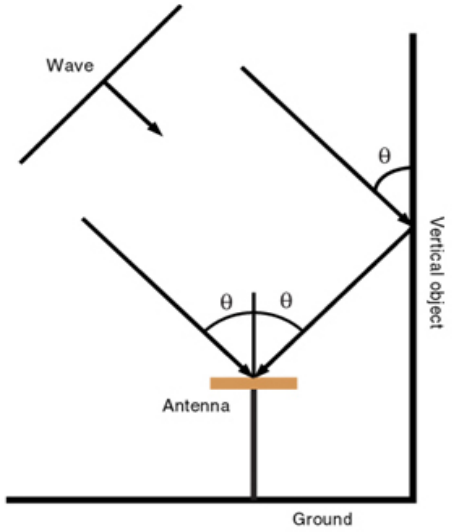

Fig. B. Reflections from vertical

antenna (LeicaAR25 GNSS) and Trimble Zephyr antenna (TRM 39105.00) are summarized in the Tables (1- 4). The processed IPWV with actual observations for choke ring and patch antenna are shown in Figs. 1&2. The various graphical plots for signal strengths and Signal to Noise Ratio (SNR) for both the frequencies (L1 & L2) are shown in Figs. 3 to 10. The plots from Figs. 3 to 6 are for Leica 3D Choke ring AR25 GNSS antenna and plots from Figs. 7 to 10 are for Trimble Zephyr antenna, 2D antenna. All antennas are omni-directional. It has been clear from the observed analysis of the data that the data gaps, cycle slips are least in Leica 3D Choke ring antenna.

3.1. *Leica choke ring antenna (AR25)*

AR25 choke ring geodetic antenna cover the entire frequency range for GPS L1, L2 and L5, GLONASS L1, L2, GALILEO L1, E5, E6 bands. The use of choke ring ground plane is typical in geodetic antennas. These allow good gain pattern control, excellent multi-path suppression, high front-to-back ratio and good AR at low elevation angles. Choke rings contribute to a stable phase center. And Leica AR25 is the best usable antenna for the high-end geodetic applications.

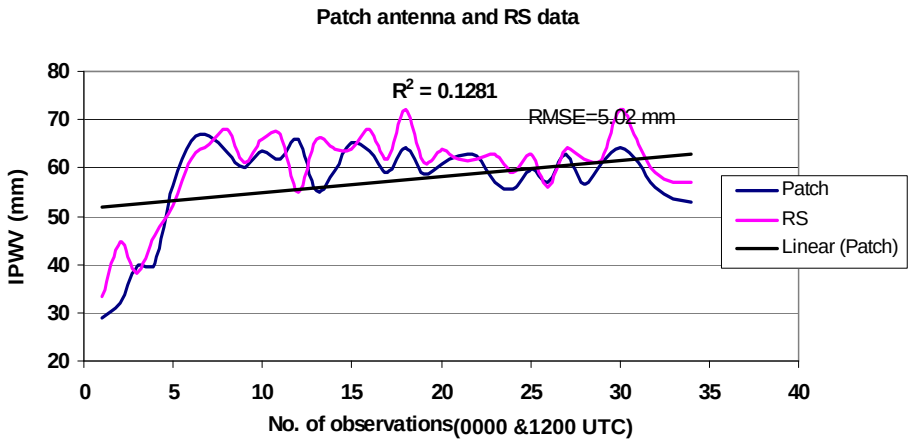

Fig. 2. IPWV (mm) processing results by Patch antenna with RS data

3.2. *Multi-path effect*

Multi-path reflections from ground (Fig. A) and from vertical can introduce (Fig. B) extra path length and introduce an error in the actual estimation of range from the GPS satellites. Positional accuracy is improved by using the choke ring antenna. Due to multi-path the probability of the false signals increased, which will generate the false IPWV estimation or abnormal values which can give bad indication of water vapour content in the atmosphere. From the ground more than one reflected signals generate false impression. Antenna design is such that it has good front to back ratio which minimizes the ground noise pickups, as RHCP antenna has by nature an LHCP response in the anti-bore sight. The front to back ratio is the difference of bore sight gain and anti-bore sight gain. Multi-path susceptibility of an antenna can be quantified with respect to the antenna's gain pattern characteristics by the multi-path ratio (MPR). MPR for ground reflections are given below:

$$MPR = \frac{E_{RHCP}(\theta)}{E_{RHCP}(180° - \theta) + E_{LHCP}(180° - \theta)} \qquad (1)$$

In the above equation (1) the reflected signals have more Left Handed Circularly Polarized (LHCP) component than Right Handed Circularly Polarized Light (RHCP). In this case the antenna gain is suitably adjusted with the help of MPR and by making the proper design of antenna (Orban and Moernaut, 2009).

Similarly the vertical reflections are minimized by suppressing the reflections of multiple objects by suitably adjusted the MPR.

$$MPR = \frac{E_{RHCP}(\theta)}{E_{RHCP}(\theta) + E_{LHCP}(\theta)} \qquad (2)$$

The good Axial Ratio (AR) of the antenna suppresses the multipath signals reflections from vertical objects, such as buildings, towers etc.

The typical multi-path error in the pseudorange measurement varies from about 1 m to 5 m. Multi-path in the pseudorange measurements are usually two orders of magnitude larger than the multi-path errors in the carrier-phase measurements (Misra and Enge, 2001; Langley, 1998).

For a receiving antenna, antenna gain is the ratio of the power delivered by the antenna in response to a signal arriving from a given direction compared to that delivered by a hypothetical isotropic reference antenna. The spatial variation of an antenna's gain is referred to as the radiation pattern or the receiving pattern. Actually, under the antenna reciprocity theorem, these patterns are identical for a given antenna. The receiver operates best with only a small difference in power between the signals from the various satellites being tracked and ideally the antenna covers the entire hemisphere above it with no variation in gain. This has to do with potential cross-correlation problems in the receiver and the simple fact that excessive gain roll-off may cause signals from satellites at low elevation angles to drop below the noise floor of the receiver.

Space borne systems at L-Band typically use circular polarization (CP) signals for transmitting and receiving and satellites orbit the Earth does not cause polarization fading as it does with linearly polarized signals and antennas. Furthermore, circular polarization does not suffer from the effects of Faraday rotation caused by the ionosphere. Faraday rotation results in an electromagnetic wave from space arriving at the Earth's surface with a

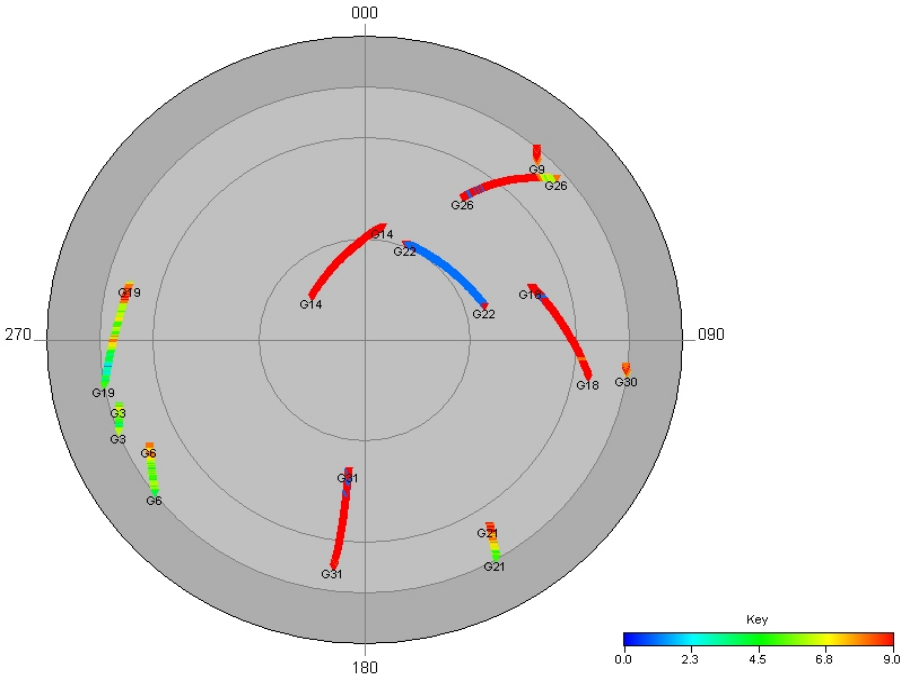

Fig. 3. L1 frequency SNR sky plot (AR25-3D Choke ring antenna)

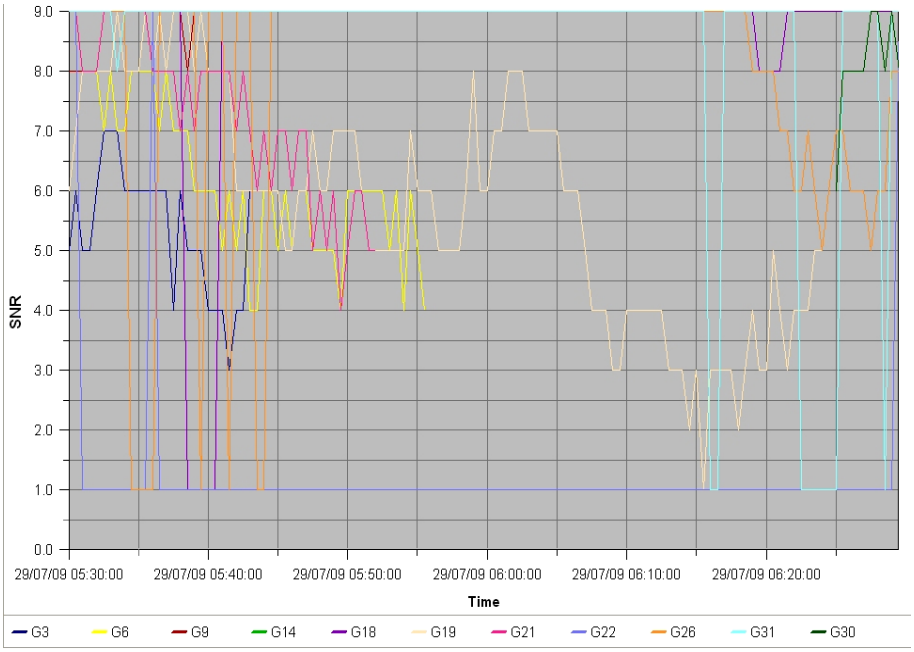

Fig. 4. L1 frequency SNR Time Series (AR25-3D Choke ring antenna)

different polarization angle than it would have if the ionosphere were absent. This leads to signal fading and potentially poor reception of linearly polarized signals. GNSS satellites use right-hand circular polarization (RHCP) and therefore a GNSS antenna receiving the direct signals must also be designed for RHCP. Antennas are not perfect and an RHCP antenna will pick up some left-hand circular polarization (LHCP) energy. LHCP part we referred as the cross-polar component.

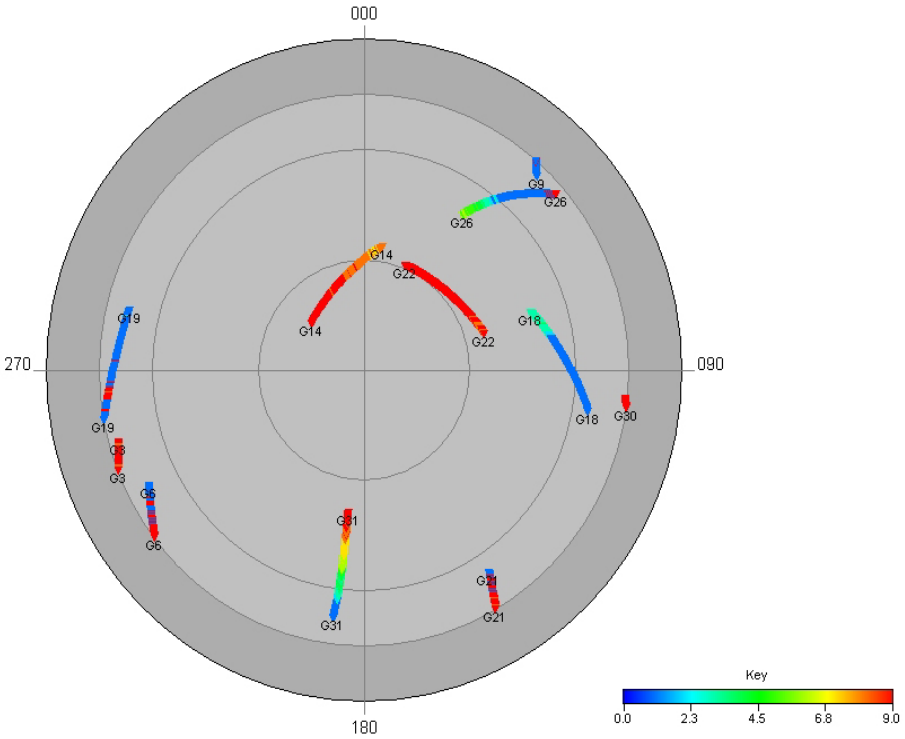

Fig. 5. L2 frequency SNR sky plot(AR25-3D Choke ring antenna)

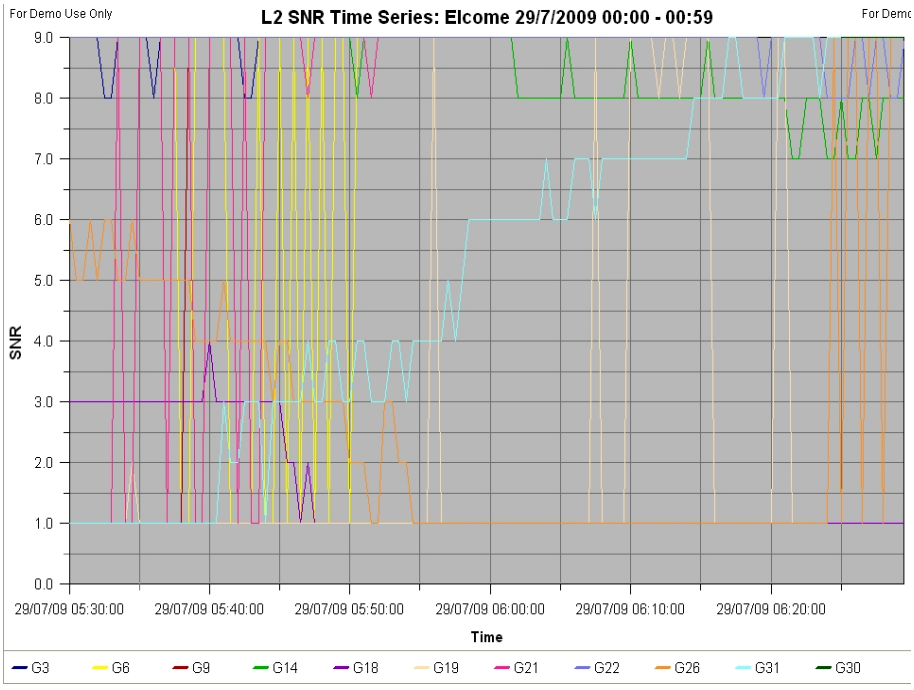

Fig. 6. L2 frequency SNR Time Series (AR25-3D Choke ring antenna)

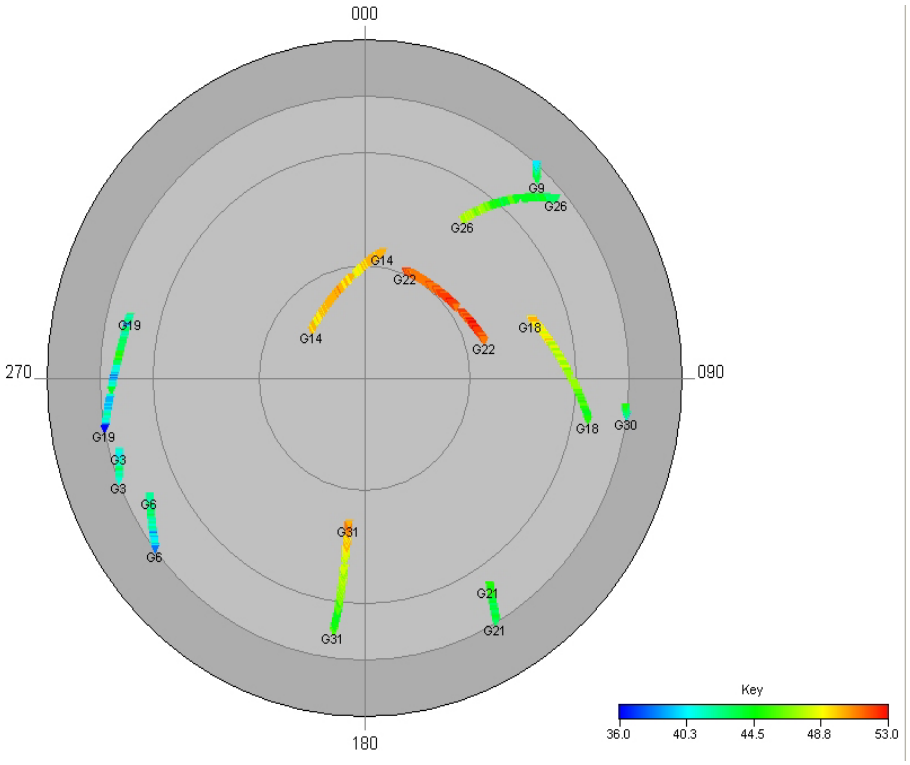

Fig. 7. L1 frequency SNR sky plot: Trimble Zephyr antenna (TRM 39105.00)

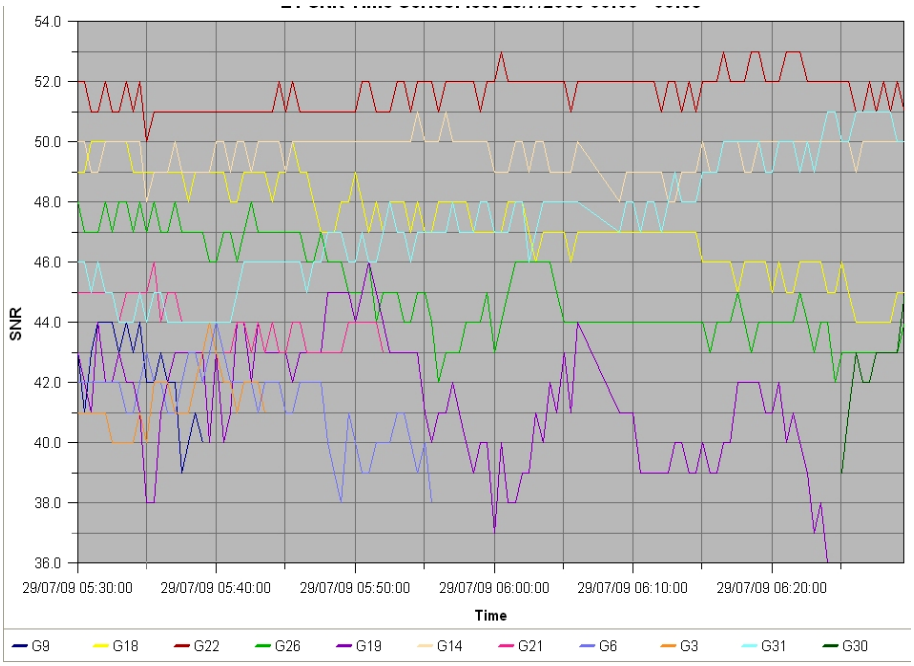

Fig. 8. L1 frequency SNR Time Series: Trimble Zephyr antenna (TRM 39105.00)

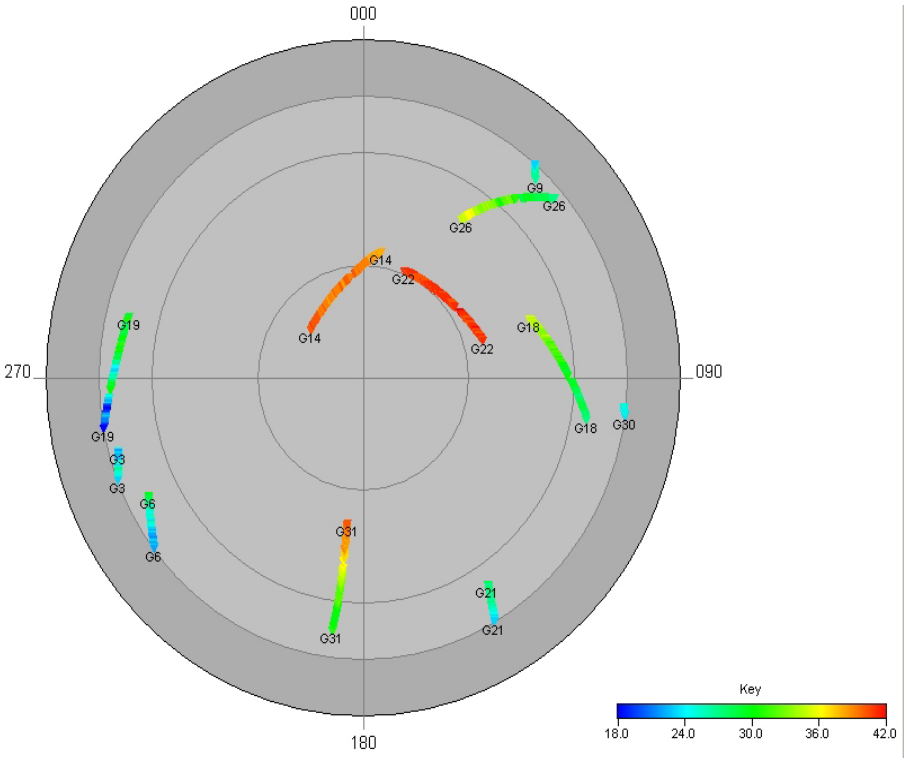

Fig. 9. L2 frequency SNR sky plot: Trimble Zephyr antenna (TRM 39105.00)

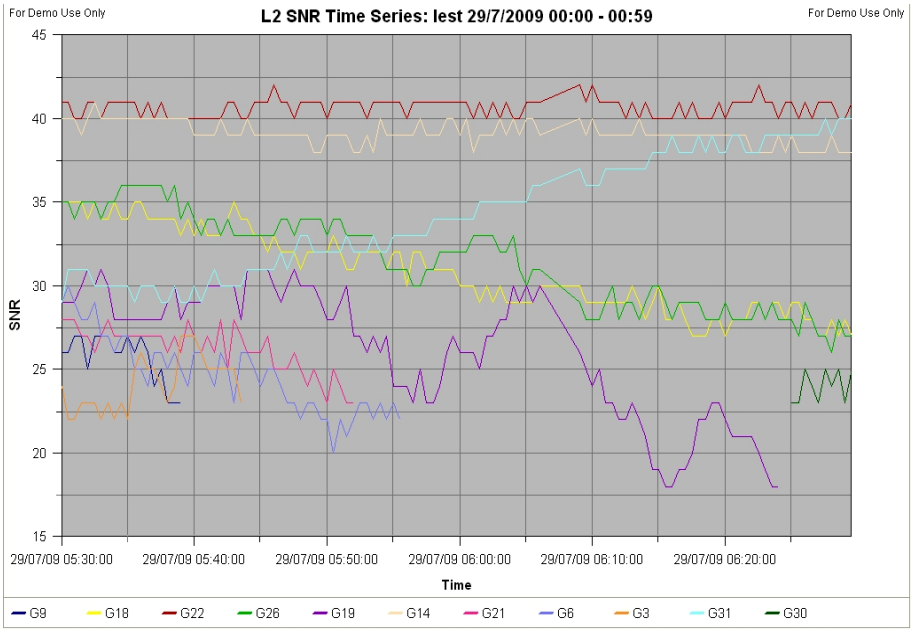

Fig. 10. L2 frequency SNR Time series: Trimble Zephyr antenna (TRM 39105.00)

Axial ratio (AR) is the measure of the polarization ellipticity of an antenna designed to receive circularly polarized signals. For high-end GNSS antennas such as choke-ring and other geodetic-quality antennas, the typical AR along the bore sight should be not greater than about 1 dB. AR increases towards lower elevation angles and you should look for an AR of less than 3 to 6 dB at a 10° elevation angle for a high-performance antenna.

The phase center is the point in space where all the rays appear to emanate from (or converge on) the antenna or it is the point where the electromagnetic fields from all incident rays appear to add up in phase. Ideally, this phase center is a single point in space for all directions at all frequencies. However, a "real-world" antenna will often possess multiple phase center points (for each lobe in the gain pattern, for example) or a phase center that appears "smeared out" as frequency and viewing angle are varied. For well-designed high-end GNSS antennas, phase center variations in azimuth are small and on the order of a couple of millimeters. The vertical phase offsets are typically 10 millimeters or less. High-performance low noise amplifier (LNA) between the antenna element itself and the receiver is required to pick up the signals from space is on the order of -130 dBm. The performance of a particular receiver element is evaluated by its noise figure (NF).

Choke-ring ground planes are typical in geodetic antennas. These allow good gain pattern control, excellent multi-path suppression, high front-to-back ratio, and good AR at low elevation angles. Choke rings contribute to a stable phase center.

3.3. *Cycle Slips*

The loss of carrier-phase tracking resulting in an integer number of cycle's discontinuity will cause an error in the carrier-phase measurements. The loss may be due to internal receiver tracking problems or an interruption in the ability of the antenna to receive the satellite signals (Seeber, 1993).

The residual phase errors due to GPS antennas will not only affect the precision in GPS networks with different types of antennas, but also in networks using identical antennas if the network covers a large spatial area (baseline lengths ~1000 km) (Schupler and Clark 1991). The performance of GPS antennas depends on the differences in the design of the antennas, manufacturing variability between antennas of the same model, the material which surrounds the antenna (including the antenna mount and radome), and the frequency range over which the antenna is used (Schupler and Clark, 2001).

3.4. *IPWV estimation*

The estimated IPWV in mm for both choke ring and patch antenna is shown in Figs. 1 & 2. The RMSE values in the case of choke ring are reduced considerably as compared to the patch antenna because patch antenna is not susceptible to suppress the multi-path effect.

3.5. *Signal to noise ratio (SNR) sky plots and its time series*

The geometry of the satellite (*i.e*., how closely or far apart satellites are spaced across the sky) is the representation of satellite availability from receiver point of view, which is graphically termed as sky plot**.** Sky plot is a plot of satellite tracks on a zenithal projection centered at the GPS ground station or it is panoramic view how the satellites are distributed. The SNR plots of L1 and L2 frequencies for Leica 3D Choke ring and Trimble Zephyr antenna are shown in Figs. 3, 5, 7 & 9. The average signal strength is represented with a color bar along with its value. The numerical values are given in Tables 1-3. The error contributions of available satellites for both frequencies are shown in Figs. 4, 6, 8 & 10.

4. Results

(*i*) The IPWV estimates are better from 3 D Choke ring antenna having R^2 = 0.1427 and RMSE = 4.36 mm as compared to patch antenna R^2 = 0.1281 and RMSE = 5.82 mm.

(*ii*) LeicaAR25 3D Choke ring antenna has better signal strength and suppression of multi-path effects as compared to the LeicaX1202, and Trimble TRM 39105.00.

(*iii*) Data gaps, cycle slips are lesser in LeicaAR25 3D Choke ring antenna as compared to LeicaX1202, and Trimble TRM 39105.00.

(*iv*) The number of observations or Epoch is more in case of LeicaAR25 3D Choke ring antenna.

(*v*) LeicaAR25 3D Choke ring antenna supports the multi-constellation with optimum accuracy.

References

Daniel, Orban and Gerald, J. K. Moernaut, 2009, "Innovation: GNSS Antennas" *GPS World*, **1**, 23-29.

Estey, L. H and Meertens, C. M.,1999, "TEQC The Multi-Purpose Toolkit for GPS/GLONASS Data, L GPS Solutions (pub. by John Wiley & Sons), **3**, 1,42-49.

Langley, R. B., 1998, "A Primer on GPS Antennas" *GPS World*, **9**, 7, 50-54.

Misra, P. and Enge, P., 2001 "Global Positioning System : Signals, Measurements, and Performance" Ganga-Januma Press, Lincoln, Massachusetts, 390.

Schupler, B. R. and Clark, T. A., 1991 "How Different Antennas Affect the GPS Observable", *GPS World*, **2**, 10, 32-36.

Schupler, B. R. and Clark, T. A., 2001, "Characterizing the Behavior of Geodetic GPS Antennas", *GPS World*, **12**, 2, 48-55.

Seeber, G., 1993, "Satellite Geodesy: Foundations, Methods and Applications" Walter de Gruyter, Berlin New York, p531.